

Synthesis, characterization and electrical properties of microtubules of polypyrrole synthesized by a template-free method

Jing Liu and Meixiang Wan*

Center for Molecular Sciences, Institute of Chemistry, Chinese Academy of Sciences, Beijing 100080, China. E-mail: wanmx@infoc3.icas.ac.cn

Received 4th October 2000, Accepted 14th November 2000

First published as an Advance Article on the web 10th January 2001

Tubular polypyrrole (PPy) doped with β -naphthalenesulfonic acid (β -NSA) was synthesized by a template-free method. SEM and TEM images proved the tubular morphology. It was found that the morphology of the resulting PPy-NSA was significantly affected by the concentration of β -NSA. When the concentration of β -NSA was increased a variation in the morphology of PPy-NSA of grain-tube-block was observed that was related to the hydrotropic behavior of β -NSA. A growth process of grain-short tube-long tube was observed, and it was assumed that polypyrrole gradually and orderly aggregated to form tubular PPy-NSA due to the acidity of the pyrrole monomer. Elemental analysis, FTIR and X-ray diffraction characterized the molecular structure of the resulting PPy-NSA. It was shown that the polymer main chain of the tubular PPy-NSA was identical to that of PPy synthesized by a common method. The differences in tubular formation mechanism and crystallinity between polyaniline (PANI)-NSA and PPy-NSA microtubules were discussed based on the basicity or acidity of the pyrrole and aniline monomers.

Introduction

Since the discovery of carbon nanotubes (CNT),¹ nanotubes or molecular wires of conducting polymers have attracted considerable attention because of their unique properties as molecular wires and potential applications in molecular devices. Among the conducting polymers, polypyrrole (PPy) is an excellent candidate for molecular wires because of its high conductivity and stability in air. Recently, template-synthesis methods²⁻⁵ and electrochemical polymerization with a scanning micro-needle electrode⁶ have been used to prepare micro- or nano-tubes and nanofibers of PPy. Meanwhile, Wan *et al.*⁷ created a template-free method to synthesize microtubules of polyaniline (PANI)⁸ and PPy.⁹ Obviously, the new method is simple and cheap, compared with the above mentioned methods, as this method omits the use of a microporous membrane acting as a template and the need for expensive apparatus.

The purpose of this article is to study the influence of the concentration of β -naphthalenesulfonic acid (naphthalene-2-sulfonic acid, β -NSA) dopant on the morphology and molecular structure of as-synthesized PPy-NSA. The tubular formation mechanism of PPy-NSA is investigated by measuring SEM images at different polymerization stages.

Experimental

Pyrrole was distilled under reduced pressure. Ammonium persulfate (APS) as oxidant and β -NSA were used without any purification.

The synthesis of PPy-NSA in this study was similar to the previous method.⁹ In a typical polymerization, 5.8×10^{-3} M pyrrole and 8×10^{-3} M β -NSA were dissolved in 8 ml deionized water with stirring. This mixture was then cooled in an ice bath. 6.7 ml of APS (0.52 M) as an oxidant was slowly added into the above mixture. The mixture was allowed to react for 10 h, and was then filtered. The residue was washed with water and methanol several times, and finally dried under vacuum at room temperature for 24 h. The tubular morphology of the resulting PPy-NSA was confirmed by scanning

electron microscopy (SEM) measurement and further proved by transmission electron microscopy (TEM). SEM and TEM were carried out on a Hitachi-530 and JEM-200CX, respectively. Elemental analysis, FTIR (Perkin-Elmer System) and X-ray diffraction (RINT 2000 wide-angle goniometer) characterized the molecular structure of the PPy-NSA. The conductivity at room temperature was measured by a four-probe method using a Keithley 196 SYSTEM DMM digital multimeter and ADVANTEST R6142 programmable DS voltage/current generator as the current source.

Results and discussion

1. Morphology and conductivity

It was found that the β -NSA concentration strongly affected the morphologies of PPy-NSA as shown in Fig. 1. When the β -NSA concentration was lower, about 0.2 M, the resulting PPy-NSA was granular (see Fig. 1a), like polypyrrole synthesized without β -NSA; when the β -NSA concentration increased, more and more fibers appeared. Finally fibers became the dominant morphology (see Fig. 1b and c). However when the concentration of β -NSA reached 2.9 M, blocks took the place of fibers (see Fig. 1d). Interestingly TEM measurements proved that those fibers were hollow. A typical TEM image of the cross-section of PPy-NSA microtubule is shown in Fig. 2. The result was similar to our previous report.⁹

In contrast, the concentration of the pyrrole monomer hardly influenced the morphology of PPy-NSA. The morphology of PPy-NSA did not change greatly, for example, when the concentration of pyrrole monomer increased from 0.54 M to 1.09 M. Thus, these results indicated that selecting an appropriate concentration of β -NSA was the key to synthesizing tubular PPy-NSA by a template-free method. The change of morphology with the concentration of β -NSA could be related to the hydrotropic behavior of β -NSA, which will be discussed in the section on formation mechanism.

Moreover, the influence of the concentration of β -NSA on the room-temperature conductivity of PPy-NSA was determined, and the results are given in Table 1. As can be seen,

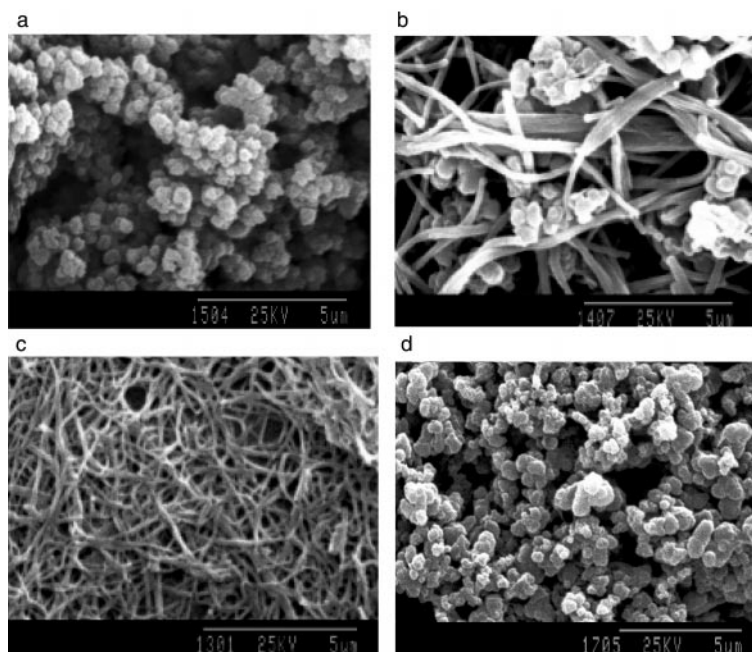


Fig. 1 SEM images of PPy-NSA synthesized under reaction conditions: [pyrrole]=0.73 M, [APS]=0.52 M, [monomer]/[oxidant]=1.67, reaction time=10 h, temp.=0 °C, [β-NSA] a. 0.2 M; b. 0.4 M; c. 1.0 M; d. 2.9 M.

there was no difference in conductivity when the concentration of β-NSA changed from 0.2 M to 1.0 M, for instance; conductivity only fluctuated from 6.3 S cm^{-1} to 2.0 S cm^{-1} . On the other hand, it dropped dramatically by three orders of magnitude when the concentration of β-NSA was raised to 2.9 M. Elemental analysis showed that the doping level, assigned as the [S]/[N] ratio, was about 0.27–0.32, no matter what concentration of β-NSA was used. This value was consistent with the normal doping level of PPy.¹⁰ Based on the elemental analysis, the conductivity of PPy-NSA should be independent of the concentration of β-NSA because of the doping levels being almost equal. However, it was only consistent with results when PPy-NSA was synthesized at low concentrations of β-NSA. Thus, what is the reason for the poor conductivity of PPy-NSA synthesized at high concentrations of β-NSA (e.g. up to 2.9 M), despite its similar doping levels (e.g. [S]/[N]=0.32)? In general, the conductivity (σ) is expressed as $\sigma = ne\mu$ where n is the density of charge carriers, e , the electronic charge and μ , the mobility of charge carriers. For a given density of charge carriers (i.e. the same doping level), the conductivity only depends on the mobility of charge carriers. Moreover, the conductivity of conducting polymers consists of chain and interchain conductivity. The former is related to transport of charge carriers along the polymer chain, while the latter is affected by the transport of charge carriers from one chain to others. In fact, the interchain transport of charge carriers significantly affects the conductivity, especially the temperature dependence of conductivity for the conducting

polymer.¹¹ For PPy-NSA synthesized at high concentrations of β-NSA (e.g. 2.9 M), the interchain transport of charge carriers was partially blocked by insulating β-NSA, which resulted in a reduction in the interchain conductivity. This was further proved by the FTIR spectra, which will be discussed later in detail.

2. Formation mechanism

In order to understand the tubular formation process of PPy-NSA, SEM images of PPy-NSA at different stages in the synthesis under optimal conditions were measured and are shown in Fig. 3. It was clearly seen that PPy-NSA exhibited a granular morphology (see Fig. 3a), when the polymerization time was about 0.5 h. After polymerization for 1.5 h, grains mixed with short fiber-like morphology in the SEM images of PPy-NSA were observed (see Fig. 3b). The short fiber-like species grew, while the grains disappeared when the reaction time was prolonged to 3.5 h (see Fig. 3c). Finally, the long fiber morphology was formed completely after polymerization for 6.5 h (see Fig. 3d). These results indicated that a growth process of grain–short tube–long tube took place in PPy-NSA. This was quite different from PANI-NSA microtubules, in which the aniline salt formed with NSA played a template-like role to form tubular PANI-NSA.^{11,12} This was because the aniline monomer was basic, and easily reacted with β-NSA to produce a salt. In the PPy system, however, the pyrrole monomer was acidic¹³ (e.g. $\text{p}K_{\text{a}}=0.4$). The difference between aniline and pyrrole is that the nitrogen atom of aniline is sp^3 hybridized and has an unshared electron pair, while that of pyrrole is sp^2 hybridized and does not have an unshared

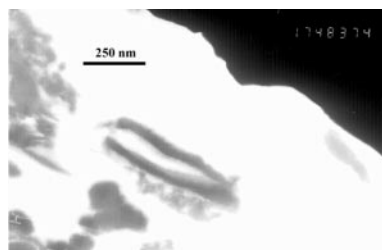


Fig. 2 TEM images of the cross-section of PPy-NSA microtubules (magnification 17×10^3) synthesized under reaction conditions: [pyrrole]=0.73 M, [APS]=0.52 M, [monomer]/[oxidant]=1.67, [β-NSA]=1.0 M, reaction time=10 h, temp.=0 °C.

Table 1 Elemental analysis and conductivity data of PPy-NSA synthesized at different concentrations of β-NSA and pyrrole

Sample	Concentration of β-NSA/M	Concentration of pyrrole/M	Conductivity/ S cm^{-1}	$N=1$ (molar)		
				C/N	H/N	S/N
1	0.2	0.73	6.25	6.56	5.15	0.27
2	0.4	0.73	6.40	6.70	5.15	0.30
3	1.0	1.09	4.77	7.02	5.46	0.30
4	1.0	0.73	2.00	6.83	5.56	0.29
5	2.9	0.73	2.02×10^{-3}	7.11	6.32	0.32

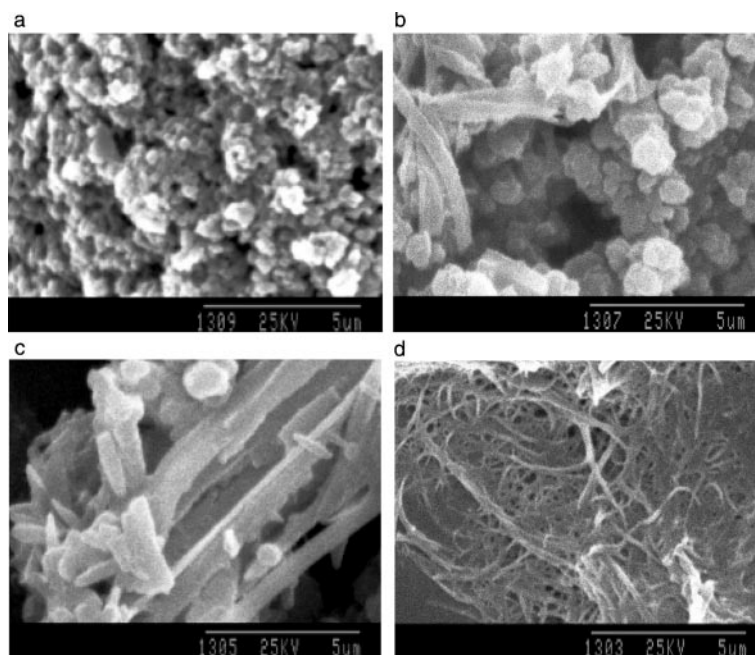


Fig. 3 SEM images of PPy-NSA synthesized under reaction conditions: [pyrrole]=0.73 M, [APS]=0.52 M, [monomer]/[oxidant]=1.67, [β -NSA]=1.0 M, temp.=0 °C, polymerization time a. 0.5 h; b. 1.5 h; c. 3.5 h; d. 6.5 h.

electron pair. As a result, the pyrrole monomer would not be expected to react with β -NSA to form a salt. This probably was the reason that the tubular formation mechanism of PPy-NSA differed from that of PANI-NSA. However, how to interpret the growth process grain–short tube–long tube for PPy-NSA synthesized by a template-free method? In fact, β -NSA was a hydrotrope, one of anionic surfactant, which increased the solubility in water of organic compounds.¹⁴ Therefore pyrrole could be dissolved in β -NSA solution. Moreover, the longer the polymerization time, the more PPy-NSA was formed. For the initial polymerization stage (*e.g.* only 0.5 h), only the granular morphology of PPy-NSA was observed because there was a lower quantity of PPy-NSA in the medium containing β -NSA. This was in agreement with the SEM images as shown in Fig. 3a. When the polymerization time increased, however, more PPy-NSA was formed in the medium of the β -NSA solution, and the formed PPy-NSA gradually aggregated in an orderly way to form fibers, which is also in agreement with results shown in Fig. 3b–d. Similarly, we also could explain the variation in morphology with the concentration of β -NSA as shown in Fig. 1, based on the hydrotropic behavior of β -NSA. Firstly, it was reasonable to believe that when the concentration of β -NSA was low, the solubility of pyrrole

monomer in the β -NSA solution was low, resulting in a granular morphology of PPy-NSA (see Fig. 1a). When the concentration was enhanced, the solubility of pyrrole dissolved in β -NSA would increase. Furthermore, β -NSA tended to form micelles in such concentrations. Therefore, the tubular PPy-NSA was easy to form in such a β -NSA medium, and this was consistent with results shown in Fig. 1c. When the β -NSA concentration was too high (*e.g.* 2.9 M), on the other hand, insoluble β -NSA and polypyrrole mixed with each other to form blocks, which is also in agreement with the results shown in Fig. 1d and with its poor conductivity.

3. Structural characterization

Fig. 4 shows FTIR spectra of PPy-NSA with different morphologies. As one can see, there are no big differences in the FTIR spectra when the morphology of PPy-NSA is changed. The characteristic bands of polypyrrole, for example, the pyrrole ring fundamental vibration centered at 1538 and 1455 cm^{-1} , the =C–H in-plane vibration at 1290, 1100, and 1030 cm^{-1} , and the N–H stretching vibration at 3400 cm^{-1} , were observed in the tubular PPy-NSA. All of those were consistent with previous reports.^{15,16} These results indicated that the polymer main chain of PPy-NSA with different

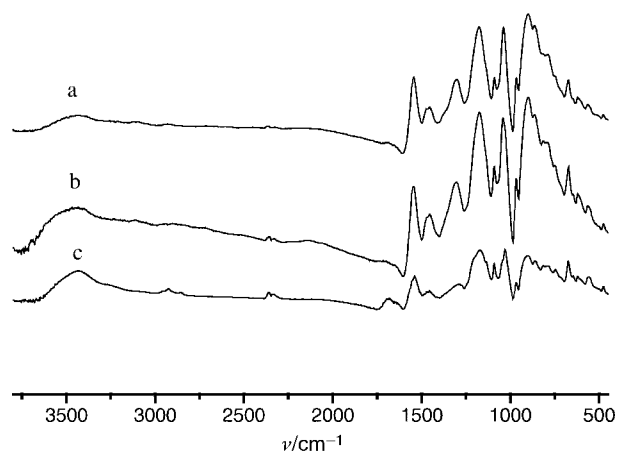


Fig. 4 FTIR spectra of PPy-NSA with different morphologies: a. tubes with more grain; b. microtubules; c. blocks.

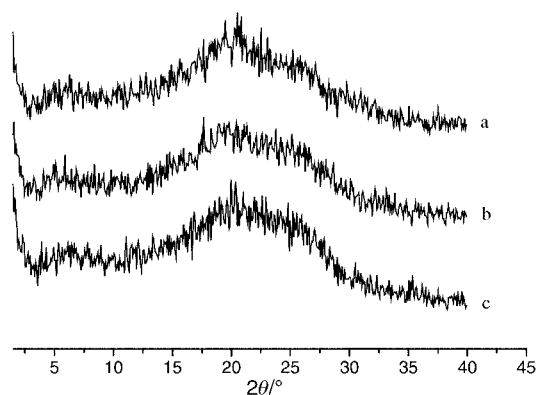


Fig. 5 X-Ray scattering patterns of PPy-NSA synthesized under reaction conditions: [pyrrole]=0.73 M, [APS]=0.52 M, [monomer]/[oxidant]=1.67, [β -NSA]=1.0 M, temp.=0 °C, polymerization time a. 3.5 h; b. 6.5 h; c. 12 h.

morphology was identical to that of PPy synthesized by a well-known method. However, it was noted that the characteristic band at 1682 cm^{-1} assigned as the pyrrolidinone carbonyl group,¹⁷ and 2923 cm^{-1} assigned as the O–H stretching vibration of the $\text{SO}_2\text{-OH}$ group in $\beta\text{-NSA}$ ¹⁷ were significantly observed when the $\beta\text{-NSA}$ concentration was too high (e.g. 2.9 M). This suggested that $\beta\text{-NSA}$ not only acted as dopant to provide counterions, but also existed in and mixed with PPy when the concentration of $\beta\text{-NSA}$ was up to 2.9 M. It is most likely that the latter increased interchain resistance due to electrical insulating $\beta\text{-NSA}$, resulting in poor conductivity (see Table 1).

Fig. 5 shows typical X-ray scattering patterns of PPy-NSA synthesized at different polymerization times. It shows that all X-ray scattering patterns were similar, and exhibited amorphous. A similar phenomenon was observed in the X-ray scattering pattern of PPy-NSA synthesized at different concentrations of $\beta\text{-NSA}$. Those results were quite different from PANI-NSA microtubules with high crystallinity.⁸ The difference in crystallinity between PPy-NSA and PANI-NSA tubules may be due to differences in the tubular formation mechanism. In the PANI system, as mentioned above, the aniline monomer reacted easily with $\beta\text{-NSA}$ to form needle-like crystals of the aniline salt, and it acted as a template for the synthesis of PANI-NSA microtubules. As a result, the resulting PANI-NSA microtubules were crystalline. In the PPy system, the pyrrole monomer could not react with $\beta\text{-NSA}$ to form a salt due to the acidity of the PPy monomer. Therefore, there was no “template” for forming PPy-NSA microtubules, so PPy-NSA gradually and orderly aggregated to form amorphous PPy-NSA microtubules.

Conclusion

(1) SEM and TEM images proved that tubular PPy-NSA could be synthesized by a template-free method in the presence of $\beta\text{-NSA}$ as a dopant.

(2) The concentration of $\beta\text{-NSA}$ greatly affected the morphology of the resulting PPy-NSA. When the concentration of $\beta\text{-NSA}$ increased, a variation in the grain–tube–block morphology took place that was related to the hydrotropic behavior of $\beta\text{-NSA}$.

(3) The room-temperature conductivity of PPy-NSA was affected by the concentration of $\beta\text{-NSA}$. For low concentrations of $\beta\text{-NSA}$ (e.g. 0.2–1.0 M), there was no influence of the concentration of $\beta\text{-NSA}$ on the conductivity, which was consistent with the doping level ($[\text{S}]/[\text{N}]=0.25$ to 0.33) measured by elemental analysis. For high concentrations (e.g. 2.9 M), however, the conductivity dropped dramatically by three orders of magnitude, although the doping level was

close to 0.32. This may be due to insulating $\beta\text{-NSA}$ blocking the interchain transport of charge carriers.

(4) Elemental analysis, FTIR and X-ray diffraction characterized the molecular structure of PPy-NSA. FTIR spectra showed that the polymer main chain of PPy-NSA was identical to that of PPy synthesized by a common method, meanwhile, X-ray diffraction measurements showed that the resulting PPy-NSA was amorphous.

(5) A growth process of grain–short tube–long tube was proved by SEM images of PPy-NSA synthesized at different polymerization stages under optimal conditions. It was assumed that polypyrrole gradually and orderly aggregated to form tubular PANI-NSA in the presence of $\beta\text{-NSA}$.

(6) The tubular formation mechanism and crystallinity of PPy-NSA differed from that of PANI-NSA, due to the acidity of the pyrrole monomer.

Acknowledgements

This project was supported by the National Natural Foundation of China (No 29634020-2 and 29974037), 973 program of China, the Center for Molecular Sciences, Institute of Chemistry, and the Chinese Academy of Sciences.

References

- 1 S. Lijima, *Nature*, 1991, **354**, 56.
- 2 Martin, *Science*, 1994, **266**, 1961.
- 3 J. C. Hulthen and C. R. Martin, *J. Mater. Chem.*, 1997, **7**, 1075.
- 4 J. Duchet, R. Legras and S. Demoustier-Champagne, *Synth. Met.*, 1998, **98**, 113.
- 5 S. Demoustier-Champagne and R. Legras, *J. Chim. Phys.*, 1998, **95**, 1200.
- 6 S. S. Shiratori, S. Mori and K. Ikezaki, *Sens. Actuators B*, 1998, **49B**, 30.
- 7 M. X. Wan, Y. Q. Shen and J. Huang, *CN Patent*, 981099165, 1998.
- 8 J. Huang and M. X. Wan, *J. Polym. Sci., Part A: Polym. Chem.*, 1999, **37**, 1277.
- 9 Y. Q. Shen and M. X. Wan, *J. Polym. Sci., Part A: Polym. Chem.*, 1999, **37**, 1443.
- 10 E. M. Genies and A. A. Syed, *Synth. Met.*, 1984, **21**, 10.
- 11 M. X. Wan, *Chinese J. Polym. Sci.*, 1995, **13**, 1.
- 12 M. X. Wan and J. C. Li, *J. Polym. Sci., Part A: Polym. Chem.*, 2000, **38**, 2359.
- 13 G. M. Badger, in *The Chemistry of Heterocyclic Compounds*, Academic Press Inc., New York and London, 1961, p. 11.
- 14 G. Hons, in *Anionic Surfactant organic chemistry*, Vol. 56, eds. Helmut W. Stache, Marcel Dekker, Inc., New York, 1995, p. 82.
- 15 W. R. Salanak, R. Erlandsson, J. Priza, I. Lundstrom and O. Inganas, *Synth. Met.*, 1983, **5**, 125.
- 16 Watanabe, M. Tanaka and J. Tanaka, *Bull. Chem. Soc. Jpn.*, 1981, **54**, 2278.
- 17 L. Chierici and G. P. Gardini, *Tetrahedron*, 1966, **22**, 53.